This manuscript was accepted by Appl. Phys. Lett. Click here to see the version of record.

Piezo-electrical control of gyration dynamics of magnetic vortices

M. Filianina,[1,2] L. Baldrati,[1] T. Hajiri,[3] K. Litzius,[1,2,4] M. Foerster,[5] L. Aballe,[5] and M. Kläui[1,2,a)]

[1)]*Institute of Physics, Johannes Gutenberg University, 55128 Mainz, Germany*

[2)]*Graduate School of Excellence Material Science in Mainz, 55128 Mainz, Germany*

[3)]*Department of Material Physics, Nagoya University, 464-8603 Nagoya, Japan*

[4)]*Max Planck Institute for Intelligent Systems, 70569 Stuttgart, Germany*

[5)]*ALBA Synchrotron Light Facility, 08290 Barcelona, Spain*

(Dated: 9 July 2019)

In this work we first statically image the electrically controlled magnetostatic configuration of magnetic vortex states and then we dynamically image the time-resolved vortex core gyration tuned by electric fields. We demonstrate the manipulation of the vortex core gyration orbit by engineering the magnetic anisotropies. We achieve this by electric fields in a synthetic heterostructure consisting of a piezoelement coupled with magnetostrictive microstructures, where the magnetic anisotropy can be controlled by strain. We directly show the strong impact of the tailored anisotropy on the static shape of the vortex state and the dynamic vortex core orbit. The results demonstrate the possibility of using electric field induced strain as a low-power approach to tune the dynamical response of magnetic vortices.

Magnetic vortices[1,2] are chiral magnetic structures with high stability and unique gyration dynamics that make them a promising candidate for information carriers in potential spintronic application like data storage[3] or for nano-oscillators.[4] Their advantage stems from the four-fold degeneracy of the magnetization configuration that makes it possible to manipulate the vortex properties independently in both the circulation direction in the plane and the out-of plane vortex polarity, thus potentially storing 2 bits.[3,5]. Recent investigations show that magnetic vortices can be effectively driven by spin currents, magnetic fields, or electric currents.[6–11] However, for each driving mechanism, the reliable motion of the vortex and manipulation of its displacement is dependent on the knowledge of its eigenmode dynamics on short temporal and spatial scales.

Conventionally one can tailor the vortex core dynamics by varying the geometry.[12,13] This approach is however limited as the geometry cannot be tailored once the structure is fabricated, while tuning the resonance frequency and vortex core trajectory on the fly is a key requirement for both tunable oscillators and efficient vortex core switching.[11] For the latter, for instance in an array of vortices one needs to address a single vortex. This switching of a selected single vortex could be achieved in a global field excitation of a fixed frequency by bringing only one selected vortex into and out of resonance for that fixed frequency excitation in a low-power approach. This will only switch this one vortex that was brought into resonance.

A flexible way for the manipulation of the vortex core gyration orbit and resonance frequency is the modulation of the particular anisotropy in the material.[14] This can be done by combining piezoelectric elements with magnetostrictive ferromagnetic structures to set the anisotropy by means of magneto-elastic (ME) coupling. Such a synthetic heterostructure provides a natural way to control the magnetization dynamics by electric fields applied to the piezoelectric element eliminating the need for applying current-intensive magnetic fields.

a)Electronic mail: klaeui@uni-mainz.de.

Being of interest for both fundamental and applied research, the quasi-static behavior of the ME coupling has been thoroughly analyzed,[15–17] however there are only few experimental studies that assess the effect of this coupling on the dynamical behavior of the magnetization, especially at the micro- and nanoscale.[14,18]

Moreover the existing studies predict fundamentally the feasibility of using ME anisotropy to modify a vortex state and its dynamics, but an experimental realization of this approach is still elusive. For practical applications a full electrical control of dynamical response of magnetic vortices is desired.

In this paper, using time-resolved x-ray magnetic microscopy, we experimentally demonstrate that electric field induced strain, acting via the ME anisotropy on magnetostrictive microstructures, not only modifies the static magnetic configurations of the microstructures, but also allows for control of the vortex core gyration dynamics.

In Fig. 1 (a, b) we schematically depict the sample environment employed in the experiment, containing a coplanar wave guide fabricated on top of a bare one-side polished commercial piezoelectric $[Pb(Mg_{0.33}Nb_{0.66}O_3)]_{0.68}$-$[PbTi_3]_{0.32}(011)$ (PMN-PT) single crystal substrate. The strain generated by applying a field for this type of substrate has been previously quantified.[19] The crystallographic directions of the PMN-PT substrate, defining the strain character, i.e. tensile and compressive for the [01-1] and [100] directions, respectively,[19] are indicated. Figure 1 (c) shows the scanning electron microscopy (SEM) image of the top surface of the investigated sample with an array of Ni microstructures of 1 μm in diameter and 50 nm in thickness on top of the Au strip line.

The magnetic configuration of the discs was investigated by means of photoemission electron microscopy (PEEM) combined with x-ray magnetic circular dichroism (XMCD).[20] For the imaging of the microstructures we used circularly polarized light at the energy of 852.5 eV, which corresponded to the Ni L_3 absorption edge. The imaging was carried out at room temperature at the CIRCE beamline at ALBA, Barcelona equipped with an Elmitec PEEM/LEEM microscope.[21]

The piezoelectric strain vs electric field response exhibits a hysteretic behavior. However, once the coercive field is overcome and the substrate is poled, the response is linear. This

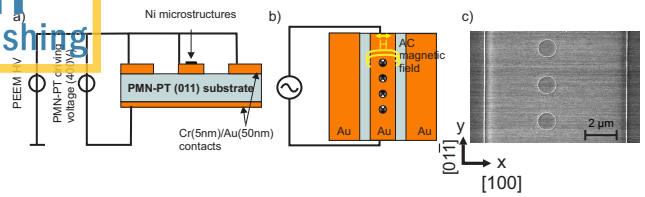

FIG. 1. (a) - Schematic of the side and (b) - the top view of the sample environment used for the observation of vortex core gyration dynamics modulated by the ME coupling. (c) - SEM image of the sample surface showing the magnetic microstructures fabricated on top of a stripline, which in turn generates an oscillating magnetic field due to the injected AC current with 500 MHz frequency. The co-planar waveguide together with the stripline and the magnetostrictive microstructures are fabricated on top of a piezoelectric substrate (with an additional electrical contact at the bottom) to generate uniaxial in-plane strain upon application of an electric field across the substrate.

allows for a full and reliable control of the generated strain by varying the applied field in the range of -100 - 600 kV/m.[19] For these magnitudes of the electric field the expected strain is in the order of 500 ppm.[19] As the total thickness of the layers between the PMN-PT and the magnetic microstructures is limited to 55 nm a complete transfer of the generated strain from the substrate to the microstructures is occurring.[16]

The motion of magnetic vortices was excited by a continuous in-plane alternating magnetic field in the x direction, generated by a sinusoidal current passed through the Au stripline (Fig. 1 (b)) at a fixed frequency of 500 MHz, which is the frequency of the synchrotron clock, set by the temporal structure of the x-ray beam.[22] The time-resolved study of the vortex core gyration was carried out by XMCD-PEEM imaging of the microstructures at different time delays of the AC excitation relative to the incoming x-rays.

Prior to XMCD-PEEM imaging of the magnetic configuration of the microstructures we *ex-situ* demagnetized the system by applying an alternating magnetic field with an exponentially decreasing amplitude using an electromagnet. For a wide range of lateral dimensions of the microstructures a vortex state was formed with the in-plane magnetization curling around a vortex core. Fig. 2 (c) shows the image of the magnetic domain structure of the 1-μm Ni disc, that was subsequently used for the time-resolved experiment. Such symmetric distribution of the domains corresponds to unstrained, shape-anisotropy dominated states.[1,2]

When an electric field is applied to the piezoelectric substrate the domain distribution in the Ni structures changes. Two magnetic domains with antiparallel magnetization alignment grow in size at the expense of the two others, with the magnetization pointing in the perpendicular direction. This indicates that the electric field induced piezoelectric strain generates a uniaxial anisotropy in the magnetic material, favoring one magnetic domain direction over the perpendicular direction domain.[16]

Note, however, that the symmetric domain distribution corresponds to an applied electric field of about 250 kV/m. This indicates the presence of an additional uniaxial anisotropy contribution at zero applied strain as previously observed.[16] A possible explanation stems from the substrate, which in its virgin state falls into a piezoelectric multidomain state.[19] When the substrate is electrically poled, regions with different piezoelectric domains may give rise to regions with a different pre-strain, which can then influence the magnetization of the Ni microstructures, fabricated on an unpoled substrate.[16] A larger compressive strain along the x direction is generated upon increasing the electric field above 250 kV/m (see Supplementary Material). Consequently, the areas of the black and white domains in Fig. 2 (d) each increase by ca. 11%. For the electric fields below 250 kV/m the compression along the x direction is weaker than that at 250 kV/m, whilst the extension along the y is stronger, as suggested by the linear response of the generated strain on the electric field.[19] Therefore the effective tensile and compressive strain acting on the Ni microstructures invert when the electric field decreases below 250 kV/m, as indicated by green and yellow arrows in Fig. 2.

Thus, domains with the magnetization along the effective compressive strain direction grow. This behavior is in line with the expected behavior of Ni with its negative magnetostrictive constant (for bulk Ni, $\lambda \sim$ -32 ppm[23]) and agrees well with the results reported earlier for microstuctured Ni squares[16].

Micromagnetic simulations were carried out in the MicroMagnum framework[24] to quantify the induced magnetoelastic anisotropies using the following parameters for Ni: exchange constant, $A = 8{\cdot}10^{-12}$ Jm^{-1}, saturation magnetization, $M_s = 4.8{\cdot}10^5$ Am^{-1} and the Gilbert damping parameter α = 0.01. The numerical discretization used for the calculations uses a cell size of 3 nm in the in-plane direction and 50 nm in the out-of-plane direction, which corresponds to the thickness of the Ni microstructures.

The effect of the electric field induced strain was introduced into the simulations as an additional uniaxial ME anisotropy term. For every value of the ME anisotropy the magnetic configuration was initialized in the vortex state and relaxed into its equilibrium state. We compared the simulated domain structures for a range of anisotropies, shown in Fig. 2 (e)-(h), with the experimental images and determined for which ME anisotropy values the domain configurations agree thereby allowing us to quantify the induced ME anisotropy.

Having established the static vortex configuration, we next address how the strain induced ME anisotropy affects the dynamical response of the magnetic vortices. Vortex core dynamics is typically excited by an in-plane magnetic field pulse on a ns-timescale, that initially forces the vortex core off-center with subsequent spiral motion back to the equilibrium position at the disk center. Alternatively, one can employ oscillating magnetic fields to excite a resonant gyration of the vortex core with the gyrotropic frequency proportional to the disk aspect ratio (L/R), where L and R are the disk thickness and radius, respectively.[11–13,25] For ferromagnetic vortices, geometrically confined in a disc, the lowest energy excitation corresponds to a periodical motion of the vortex core around its equilibrium position with a particular gyration tra-

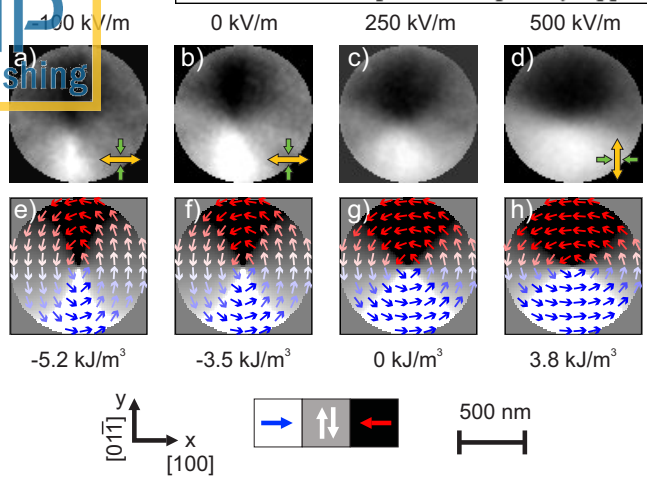

FIG. 2. (a)-(d) – XMCD-PEEM images of the magnetization configuration of a 1-μm Ni disc as a function of different applied electric fields across the piezoelectric substrate. (e)-(h) – Micromagnetically simulated magnetization configuration of a 1-μm Ni disc, introducing different magnitudes of the ME anisotropies. The gray scale indicates the magnetic contrast and the colored arrows indicate the magnetization direction.

jectory.

The dynamic gyration movement can be described in the general case by the following equation of motion:[26,27]

$$\tilde{M}\ddot{\mathbf{r}} - \mathbf{G}\times\dot{\mathbf{r}} - D\dot{\mathbf{r}} + \nabla U(\mathbf{r}) = 0, \qquad (1)$$

where $\mathbf{r}$ is the position of the vortex core, $\tilde{M}$ its effective mass tensor, $\mathbf{G}$ the gyrovector, describing the precessional motion of the vortex core, and D a dissipation term proportional to the Gilbert damping α. $U(\mathbf{r})$ is the potential energy of the vortex core with its minimum at the equilibrium position of the vortex core, corresponding to the center of the nanostructured magnetic element in the absence of external fields. By introducing additional anisotropy into the system it is possible to modify the potential energy profile $U(\mathbf{r})$ in Eq. 1, giving rise to a different and anisotropic potential, which is thus expected to affect the dynamical response of the excited vortex core.

To study the vortex core dynamics, we acquired a series of XMCD-PEEM images of 1 μm-sized Ni discs, when a current oscillating at 500 MHz was constantly flowing through the strip line, generating an alternating Oersted field and thus constantly sustaining the vortex core gyration. The *xy* position of the vortex core was then extracted from the experimental XMCD-PEEM images.

The results of the vortex core dynamics excited by an alternating magnetic field are summarized in Fig. 3 (a)-(d). The vortex core *xy* position is plotted for different times during the vortex core gyration for four given electric fields applied to the piezoelectric substrate. The data set represented by red dots in Fig. 3 (c), measured at 250 kV/m applied, is nearly circular, which corresponds to an unstrained vortex state, as discussed above (Fig. 2 (c)) and agrees with the theoretically predicted behavior.[28,29]

When the ME uniaxial anisotropy comes into play, i.e.

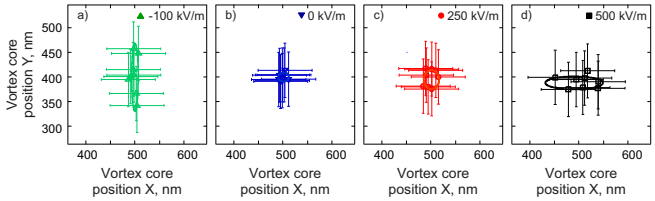

FIG. 3. (a)-(d) – Experimentally determined distribution of *xy* positions of the vortex core during its gyration measured as a function of an electric field applied to the piezoelectric substrate. The *xy* positions were extracted from the time-resolved XMCD-PEEM images using the algorithm described in detail in Supplementary Material.

when an electric field applied to the substrate is varied, the behavior deviates from a circular orbit. For positive electric fields with a higher magnitude, which induce the ME anisotropy easy axis in the Ni disc along the direction of the AC magnetic field (*x* in Fig. 2), the vortex core displacement along the *x* direction reaches ca. 90 nm, while in the *y* direction it moves within 40 nm, as represented by black square markers in Fig. 3 (d). For zero and negative applied electric fields, shown by blue and green markers in Fig. 3 (a, b), respectively, the vortex core position is confined in the *x* direction, i.e. the amplitude along *x* of its gyration does not exceed a few tens of nm. Moreover, the *xy* positions measured at -100 kV/m exhibit a stronger spread in the *y* direction, by more than 100 nm.

It follows that the application of an electric field, and thus the piezoelectric strain, strongly deforms the vortex core gyration orbit. The induced ME anisotropy confines the vortex core gyration, so that it moves along the easy ME anisotropy axis. This observation agrees with previously reported behavior.[30,31] It was theoretically shown that imposing a uniaxial anisotropy along the *x* direction in the vortex state modifies the restoring force acting on the vortex core when it is away from its central equilibrium position. The reported softening of the restoring force (which is more prominent along the anisotropy direction) determines, in particular, the eigenfrequency decrease for the distorted vortex state compared to the undistorted vortex state. Another consequence of this is the increased ellipticity of the vortex core trajectories. As shown previously, the magneto-elastically induced additional anisotropy acts as to expel the vortex core from the disc along the *x* direction.[30] In fact both these effects need to be taken into account to understand the observed modification of the vortex core gyration orbit under the application of an electric field generated strain.

To qualitatively assess the experimental results, we compared them to micromagnetic simulations of a vortex core gyration orbit for various values of the effective ME anisotropy. To be able to carry out simulations in realistic computational times with sufficient accuracy, we considered a disc of smaller dimensions, i.e. 20 nm thick with 200 nm radius, thus having the same aspect ratio as the one used in the experiment, which was relaxed into a vortex state. Note that the quantitative amplitudes of the ME anisotropy used for the these simulations are different, because of the different disc dimensions consid-

ered and the shape anisotropy that is much larger for smaller discs. The magnitudes of the induced ME anisotropy were chosen to introduce sizable changes in the magnetic configuration, analogous to the ones presented in Fig. 2 (e)-(h).

To excite the vortex core gyration in simulations we imposed an in-plane oscillating magnetic field with an amplitude of 3 mT along the x direction similar to the experimental conditions. The position of the vortex core was extracted from micromagnetic simulations by finding the xy coordinates where the absolute value of the out-of-plane component of the magnetization was maximum. First, the frequency of the excitation was set to 256 MHz, which is approximately the resonance frequency of the vortex core gyration for the undistorted vortex state and for the geometry used. The resulting vortex core gyration orbits as a function of the ME anisotropy are shown in Fig. 4 (b).

One can see that without the contribution of the ME anisotropy, i.e. when the domain structure is not distorted (similarly to Fig. 2 (g)), the gyration orbit is circular (red circular markers in Fig. 4 (b)), because the excitation occurs with the frequency that corresponds to the eingenfrequency of the system. However it becomes deformed once the ME anisotropy sets in. The amplitudes of the ME anisotropy used for the simulations are chosen to produce similar changes of the domain structure relative to the undistorted vortex configuration as in the experiments.

Additionally we performed a series of simulations, where the excitation frequency does not match the resonance frequency of the vortex core gyration for this geometry to see if the effect of the ME anisotropy is qualitatively different. The corresponding vortex core gyration orbits excited with 200 MHz and 300 MHz oscillating magnetic field in the x direction are depicted in Fig. 4 (a, c) for various amplitudes of the ME anisotropy. The selected excitation frequencies enable us to analyze two regimes, namely for frequencies well above and below the gyrotropic eigenfrequencies of both the undistorted vortex state and the state modified by the induced ME anisotropy.

By comparing the trajectories represented by red circular markers in Fig. 4 (a-c) we can clearly see the sole effect of the off-resonant excitation. As described analytically[32] and demonstrated numerically,[33] the gyration orbit becomes elongated perpendicular to the excitation field direction, if the excitation frequency is smaller than the eigenfrequency of the system (red in Fig. 4 (a)). If the excitation frequency is larger than the eigenfrequency, the orbit is elongated along the oscillating magnetic field direction (red in Fig. 4 (c)).

However, the individual effect of the ME anisotropy alone on the steady state motion of a vortex core cannot be disentangled, because the induced anisotropy also reduces the eigenfrequency of the system for the reasons mentioned earlier in the text. Thus both effects contribute to the modification of the gyration orbit.

As an example, we consider the excitation frequency that matches the eigenfrequency at zero ME anisotropy (Fig. 4 (b)). The gyration orbit of the symmetric vortex is circular because the excitation occurs at resonance. The gyration orbits at $K_{ME} = 6.8$ kJ/m^3 and $K_{ME} = -10.3$ kJ/m^3 should be on one hand both elongated in the x direction, because the excitation frequency is larger than the eigenfrequencies corresponding to the deformed states, which are 230 MHz and 208 MHz, respectively. On the other hand, the ME anisotropy also sets the preferred direction for the gyration, i.e. along x for $K_{ME} = 6.8$ kJ/m^3 and along y for $K_{ME} = -10.3$ kJ/m^3. Depending on which of these two effects is dominant, the gyration orbits can be elongated either along the x or along the y directions. Generally, by having these two effects counteracting, as for the $K_{ME} = -10.3$ kJ/m^3 in Fig. 4 (b), one can also tune the magnitude of the ME anisotropy to fully compensate these contributions and make the gyration orbit circular even when the excitation occurs off resonance.

The trends of the orbit modifications in Fig. 4 (a, c) have a similar underlying mechanism. In the first case, as the excitation occurs below the resonance, all orbits tend to align along the y direction. In addition, the uniaxial ME anisotropy along y makes the y direction even more favorable for the orbit shown by green markers, while for $K_{ME} = 6.8$ kJ/m^3, the ME anisotropy counteracts the frequency mismatch and leads for the black orbit to an elongation in the x direction. This results in the orbit at $K_{ME} = 6.8$ kJ/m^3 being more elongated along x than the orbits at $K_{ME} = -10.3$ kJ/m^3 and $K_{ME} = 0$ kJ/m^3, as it can be seen in Fig. 4 (a).

The opposite is observed when the excitation frequency is above the resonance (Fig. 4 (c)). The off-resonance excitation frequency leads to the orbit elongation along the excitation field direction, i.e. along x. The ME anisotropy in the x direction makes the orbit shown in black even more elongated along x, while the counteracting ME anisotropy in the y direction reduces the elongation along x for the orbit shown by green markers.

Thus, the micromagnetic simulations show that by means of the ME anisotropy one can tune not only the gyrotropic frequency of a system to the resonance, but also the orbit so that it acquires a circular shape even if the excitation occurs off resonance.

Even though the simulations of the dynamics were performed using a different geometry than the experimental one, the found mechanisms can explain qualitatively the experimental observations. More specifically, the experiments revealed that the gyration orbit becomes elongated in the x (y) direction for 500 kV/m (-100 kV/m) as depicted in Fig. 2, i.e. the gyration becomes more favorable in the direction of the easy axis induced by the piezoelectric strain. While being also governed by the competition between the frequency mismatch due to the ME anisotropy and the effect of the anisotropy itself, the experimentally observed modifications of the gyration orbit associated with the electrically tunable strain allow us to identify that the contribution of the ME anisotropy is dominant for the particular microstructures studied here experimentally.

To conclude, we have studied vortex core gyration dynamics in magnetostrictive microstructures fabricated on top of a piezoelectric substrate and its modification due to an electric field applied across the piezoelectric. We have found that the ME anisotropy generated by piezoelectric strain modifies the magnetic configuration of the microstructures

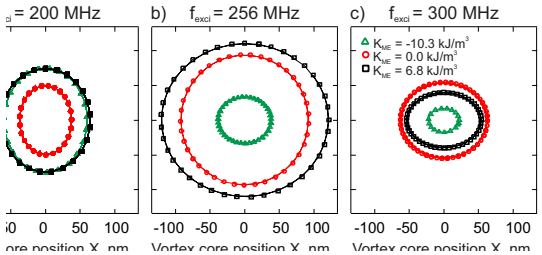

FIG. 4. Micromagnetically simulated orbits of the vortex core gyration in a 200 nm diameter 20 nm-thick Ni disc after the excitation with an in-plane magnetic field oscillating at 200 MHz, (b) 256 MHz and (c) 300 MHz with an amplitude of 3 mT for selected values of the induced ME anisotropy.

statically. In particular it also influences the vortex core gyration orbit, which we determined by time-resolved imaging of the magnetic configuration of the vortices. We have found that electrically induced and controlled ME anisotropy allows one to tune not only the gyrotropic frequency of the microstructures but also the shape of the vortex core gyration orbit. The two underlying mechanisms responsible for the observed modifications of the gyration orbit are the change in the resonance frequency and the change in the potential landscape due to the induced anisotropy. The magnetization dynamics behavior observed in the experiment is in good qualitative agreement with the micromagnetic simulations, where the effect of piezoelectric strain was modeled by an additional uniaxial anisotropy term. Our results show that electrically induced strain can be used to tailor the magnetodynamic response of magnetic vortices. Of particular importance is that the resonance frequency of a vortex can be tuned to match the excitation frequency by using electric fields. Thus, this approach provides an energy efficient tool to fully electrically control vortex dynamics which is a key asset for future vortex applications in microwave devices.

See supplementary materials for experimental details, comparison of experimental XMCD-PEEM images with micromagnetic simulations, the vortex core location algorithm and additional supporting simulations of the impact of strain on vortices.

ACKNOWLEDGMENTS

Part of this work was performed at the CIRCE beamline at ALBA Synchrotron, Barcelona, Spain. The authors further acknowledge ALBA Synchrotron staff for the technical support. The work was financially supported by the Graduate School of Excellence "Materials Science in Mainz" (MAINZ), and the Deutsche Forschungsgemeinschaft (DFG) Grant No. KL1811/18.

[1] T. Shinjo, T. Okuno, R. Hassdorf, K. Shigeto, and T. Ono, *Science* **289**, 930 (2000).
[2] A. Wachowiak, J. Wiebe, M. Bode, O. Pietzsch, M. Morgenstern, and R. Wiesendanger, *Science* **298**, 577 (2002).
[3] S. Bohlens, B. Krüger and A. Drews, M. Bolte, G. Meier and D. Pfannkuche, *Applied Physics Letters* **93**, 142508 (2008).
[4] V. S. Pribiag, I. N. Krivorotov, G. D. Fuchs, P. M. Braganca, O. Ozatay, J. C. Sankey, D. C. Ralph, R. A. Buhrman, *Nature Physics* **3**, 498 (2007).
[5] T. Uhlig, M. Rahm, C. Dietrich, R. Höllinger, M. Heumann, D. Weiss and J. Zweck, *Physical Review Letters* **95**, 237205 (2005).
[6] L. Heyne, J. Rhensius, D. Ilgaz, A. Bisig, U. Rüdiger, M. Kläui, L. Joly, F. Nolting, L.J. Heyderman, J.U. Thiele and F. Kronast, *Physical Review Letters* **105**, 187203 (2010).
[7] P. N. Skirdkov, K. A. Zvezdin, A. D. Belanovsky, J. M. George, J. C. Wu, V. Cros, and A. K. Zvezdin, *Physical Review B* **92**, 094432 (2015).
[8] G. Heldt, M. T. Bryan, G. Hrkac, S. E. Stevenson, R. V. Chopdekar, J. Raabe, T. Thomson and L. J. Heyderman, *Applied Physics Letters* **104**, 182401 (2014).
[9] M. Bolte, G. Meier, B. Krüger, A. Drews, R. Eiselt, L. Bocklage, S. Bohlens, T. Tyliszczak, A. Vansteenkiste, B. Van Waeyenberge, K. W. Chou, A. Puzic and H. Stoll, *Physical Review Letters* **100**, 176601 (2008).
[10] A. Bisig, C. A. Akosa, J.-H. Moon, J. Rhensius, C. Moutafis, A. von Bieren, J. Heidler, G. Kiliani, M. Kammerer, M. Curcic, M. Weigand, T. Tyliszczak, B. Van Waeyenberge, H. Stoll, G. Schütz, K.-J. Lee, A. Manchon and M. Kläui, *Physical Review Letters* **117**, 277203 (2016).
[11] B. Van Waeyenberge, A. Puzic, H. Stoll, K.W. Chou, Tyliszczak, R. Hertel, M. Fähnle, H. Brückl, K. Rott, G. Reiss, I. Neudecker, D. Weiss, C. H. Back and G. Schütz, *Nature* **444**, 461 (2006).
[12] K. Yu. Guslienko and B. A. Ivanov and V. Novosad and Y. Otani and H. Shima and K. Fukamichi, *Journal of Applied Physics*, **91** 8037, (2002).
[13] K. Yu. Guslienko, W. Scholz, R. W. Chantrell and V. Novosad, *Physical Review B* **71**, 144407 (2005).
[14] S. Finizio, S. Wintz, E. Kirk, A. K. Suszka, S. Gliga, P. Wohlhüter, K. Zeissler and J. Raabe, *Physical Review B* **96**, 054438 (2017).
[15] M. Weiler, A. Brandlmaier, S. Geprägs, M. Althammer, M. Opel, C. Bihler, H. Huebl, M. S. Brandt, R. Gross and S. T. B. Goennenwein, *New Journal of Physics* **11**, 013021 (2009).
[16] S. Finizio, M. Foerster, M. Buzzi, B. Krüger, M. Jourdan, C. A. F. Vaz, J. Hockel, T. Miyawaki, A. Tkach, S. Valencia, F. Kronast, G.P. Carman, F. Nolting and M. Kläui, *Physical Review Applied* **1**, 021001 (2014).
[17] M. Buzzi, R. V. Chopdekar, J.L. Hockel, A. Bur, T. Wu, N. Pilet, P. Warnicke, G.P. Carman, L. J. Heyderman and F. Nolting, *Physical Review Letters* **111**, 027204 (2013).
[18] M. Foerster, F. Maciá, N. Statuto, S. Finizio, A. Hernández-Mínguez, S. Lendínez, P.V. Santos, J. Fontcuberta, J. Manel Hernández, M. Kläui and L. Aballe, *Nature Communications* **8**, 407 (2017).
[19] T. Wu, P. Zhao, M. Bao, A. Bur, J. L. Hockel, K. Wong, K. P. Mohanchandra, C. S. Lynch and G. P. Carman, *Journal of Applied Physics* **109**, 124101 (2011).
[20] J. Stöhr, Y. Wu, B. D. Hermsmeier, M. G. Samant, G. R. Harp, S. Koranda, D. Dunham and B. P. Tonner, *Science* **259**, 658 (1993).
[21] L. Aballe, M. Foerster, E. Pellegrin, J. Nicolas and S. Ferrer, *Journal Synchrotron Radiation* **22**, 745(2015).
[22] M. Foerster, J. Prat, V. Massana, N. Gonzalez, A. Fontsere, B. Molas, O. Matilla, E. Pellegrin and L. Aballe, *Ultramicroscopy* **171**, 63 (2016).
[23] E. W. Lee, *Reports on Progress in Physics* **18**, 184 (1955).
[24] MicroMagnum, http://micromagnum.informatik.uni-hamburg.de.
[25] B. Choe, Y. Acremann, A. Scholl, A. Bauer, A. Doran, J. Stöhr and H. A. Padmore, *Science* **304**, 420 (2004).
[26] A. A. Thiele, *Physical Review Letters* **30**, 230 (1973).
[27] G. M. Wysin, *Magnetic Excitations and Geometric Confinement* (IOP Publishing, 2015).
[28] B. Krüger, A. Drews, M. Bolte, U. Merkt, D. Pfannkuche and G. Meier, *Physical Review B* **76**, 224426 (2007).
[29] D. E. Parkes, R. Beardsley, S. Bowe, I. Isakov, P. A. Warburton, K. W. Edmonds, R. P. Campion, B. L. Gallagher, A. W. Rushforth and S. A. Cavill, *Applied Physics Letters* **105**, 062405 (2014).
[30] P. E. Roy, *Applied Physics Letters* **102**, 162411 (2013).
[31] K. S. Buchanan, P. E. Roy, M. Grimsditch, F. Y. Fradin, K. Yu. Guslienko, S. D. Bader, V. Novosad, *Physical Review B* **74**, 064404 (2006).
[32] K. Yu. Guslienko, *Applied Physics Letters* **89**, 022510 (2006).
[33] K.-S. Lee, K. Yu. Guslienko, J.-Yo.-Lee and S.-K.Kim, *Physical Review B* **76**, 174410 (2007).

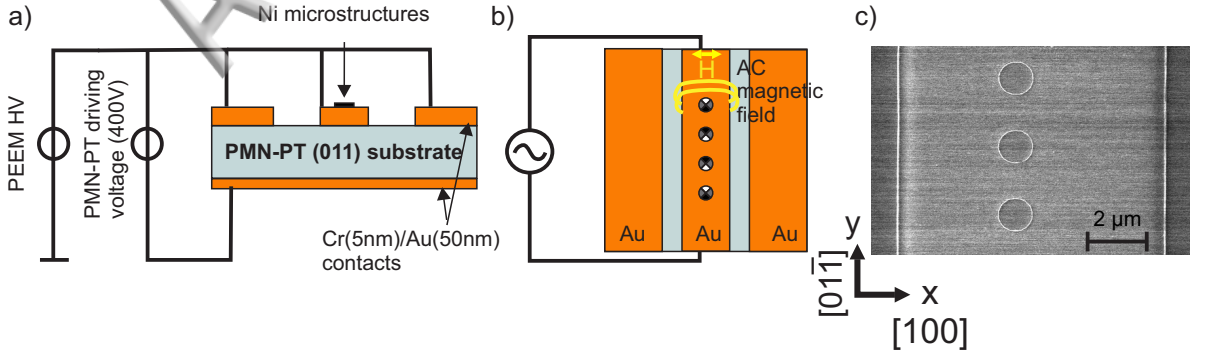
a)
Ni microstructures
PEEM HV
PMN-PT driving voltage (400V)
PMN-PT (011) substrate
Cr(5nm)/Au(50nm) contacts
b)
H
AC magnetic field
Au
Au
Au
c)
2 µm
y
x
[01$\bar{1}$]
[100]

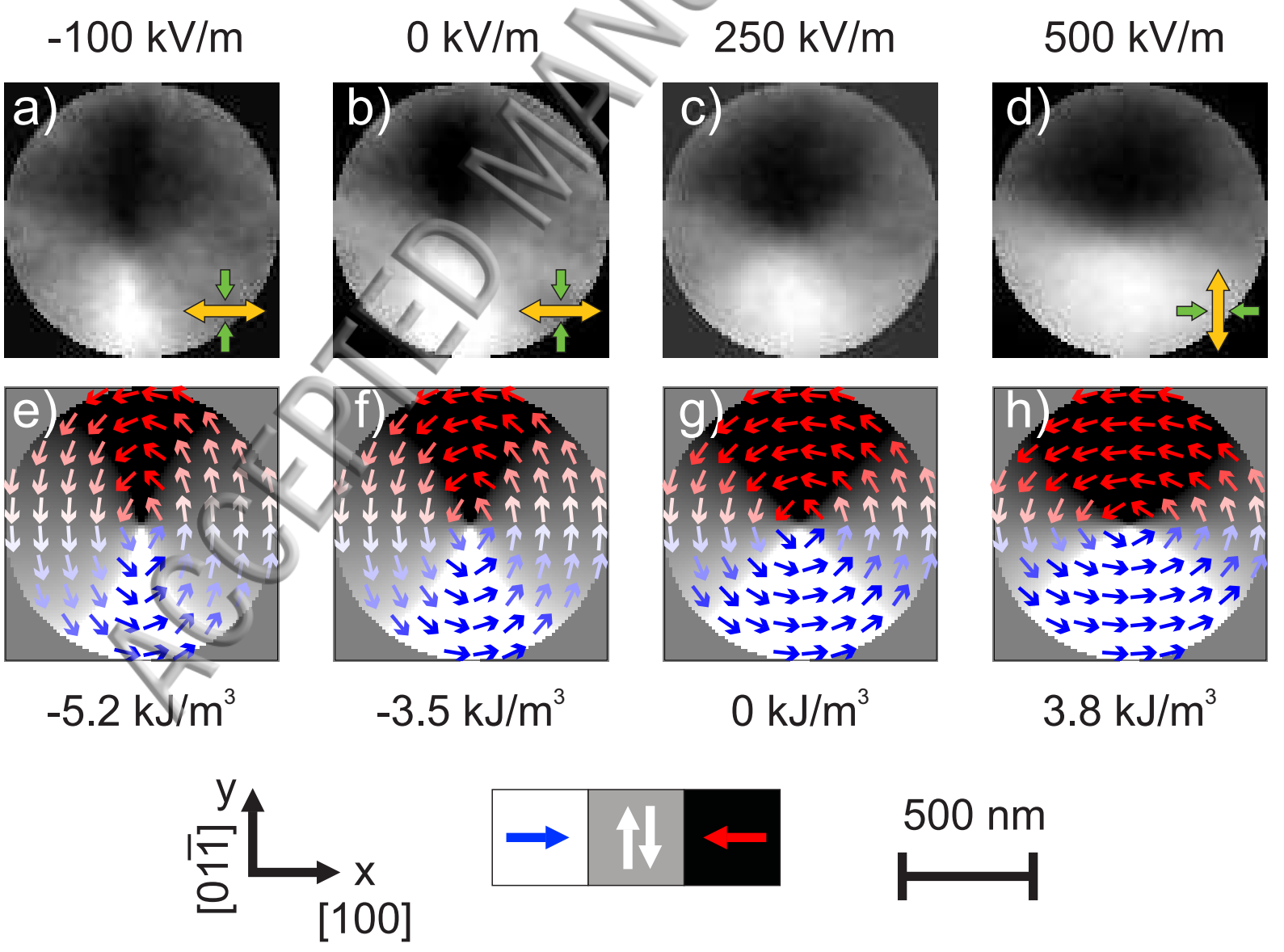

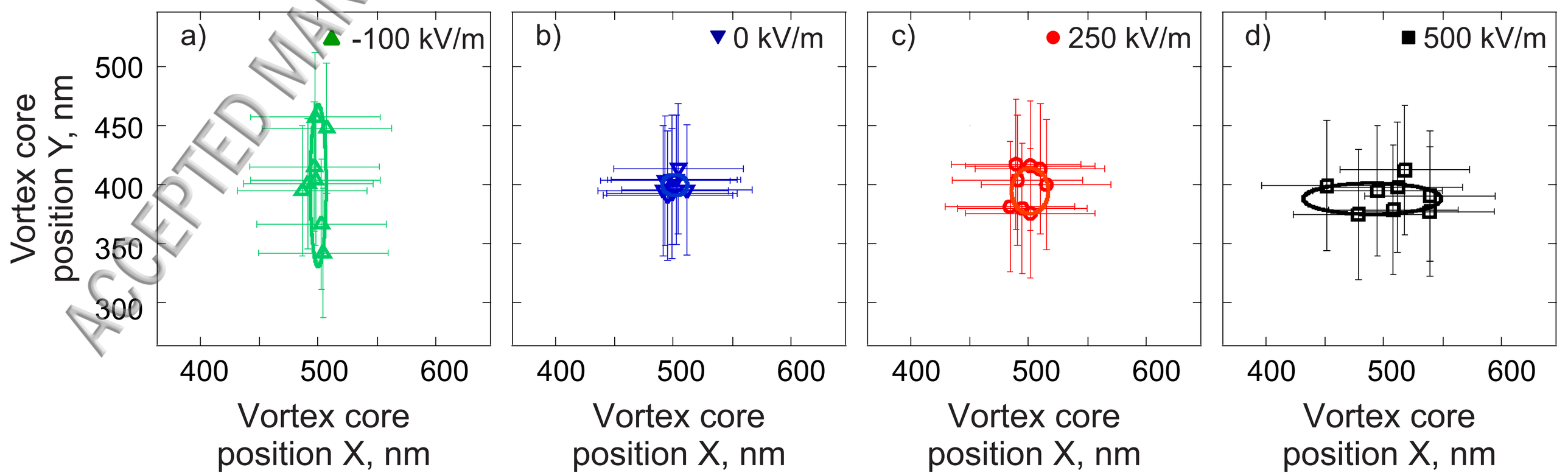

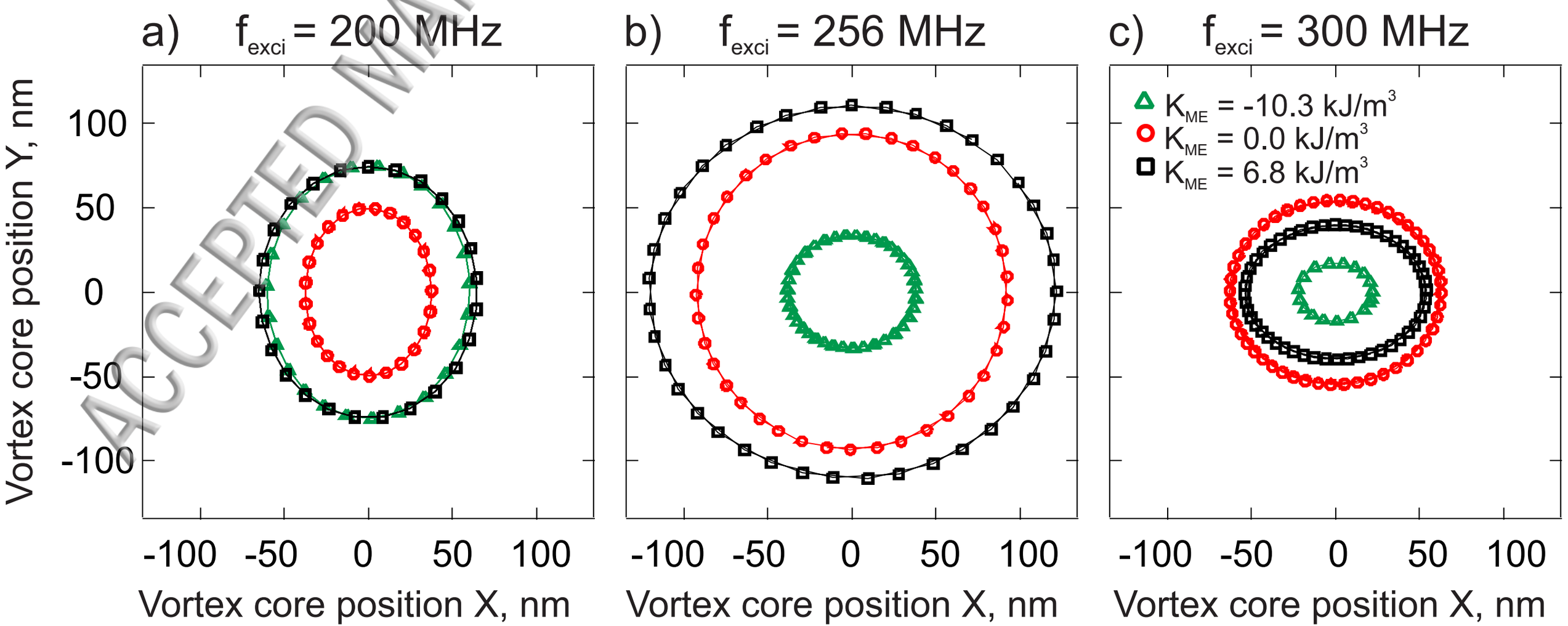
a) f_exci = 200 MHz
b) f_exci = 256 MHz
c) f_exci = 300 MHz
K_ME = -10.3 kJ/m^3
K_ME = 0.0 kJ/m^3
K_ME = 6.8 kJ/m^3
Vortex core position Y, nm
Vortex core position X, nm
Vortex core position X, nm
Vortex core position X, nm
100
50
0
-50
-100
-100 -50 0 50 100